METHODOLOGY FOR EVALUATION OF MIGRATING TYPE CORROSION INHIBITORS AND A DISCRETE ZINC SACRIFICIAL ANODE CATHODIC PROTECTION SYSTEM APPLIED ON A 30-YEAR OLD CARBONATED CONCRETE BUILDING

by

Seung-Kyoung Lee and Paul D. Krauss

Wiss, Janney, Elstner Associates, Inc.
330 Pfingsten Road
Northbrook, Illinois, 60062, USA

INTRODUCTION

Concrete possesses high pH (12.5 to 13.5) by nature and reinforcing bars embedded in concrete form a stable thin oxide film (or passive film) on the surface in the presence of such a high alkaline environment. Therefore, reinforcing bars in concrete under this environment exhibit very low corrosion rates due to the passive film. However, there are two primary corrosion mechanisms of reinforcing steel in concrete and both processes take place through destroying of the passive film (depassivation). The first type of corrosion is induced by chloride ions that attack the passive film locally and spread the depassivated area with time. The chloride-induced corrosion of reinforcing bars usually results in pitting on the bar surface and can be intensive. The second type of corrosion is caused by carbonation of the concrete. This process involves a chemical reaction between calcium hydroxide in concrete and mainly carbon dioxide in the air that lowers the pH of the concrete. As the carbonation front reaches the reinforcing bar, the passive film on the bar starts to break down at pH 10-11 and eventually becomes depassivated. When these two processes, singularly or in combination, are coupled with moisture and oxygen, corrosion of reinforcing bars in concrete proceeds at a rate which can be controlled by many factors such as dissolved oxygen availability, moisture content, resistivity of concrete, and temperature. The macrocell corrosion between macro-anode and macro-cathode can be an important factor because the anode is actively corroding at the rate of consuming electrons on the cathode. Since concrete acts as a barrier to water, chloride ions, carbonation and oxygen, the depth of cover over the bars, cracks, and permeability of concrete are also important.

A comprehensive corrosion condition survey was performed at a 30-year old office building located in Honolulu, Hawaii in 2001. The building was treated with a silane-based product approximately 12 years ago in an attempt to mitigate corrosion-induced damage. However, the product had not been effective in arresting the corrosion problem. It was determined that carbonation of concrete was responsible for the corrosion damage observed in this building and the carbonated concrete layer was near or greater than 19 mm thick in most areas at the time of the condition survey. Approximately 30 percent of the locations investigated were under the risk of the carbonation-induced corrosion. The level of chloride contamination was not high enough to initiate chloride-induced corrosion in most areas. The rate of corrosion was low and the observed corrosion morphology was general type of corrosion that is typical for bars subjected to carbonation-induced corrosion. Therefore, it was recommended that the building should be protected from on-going corrosion by applying a surface-applied migrating corrosion inhibitor.

Following the condition survey, a 6-month field testing program was launched in early 2002 involving three surface-applied migrating type corrosion inhibitors (MCI) on selected areas of the building. This phase of work was to evaluate the effectiveness of three migrating type corrosion inhibitor products for the building which was previously treated with a silane product. A discrete zinc sacrificial anode cathodic protection system was also tested for three months as a parallel investigation in an overhang trellis wall on this property. This paper discusses the results of this study.

EXPERIMENTAL

Installation of Corrosion Inhibitors

Three commercially available surface-applied migrating type corrosion inhibitors (designated Products A, B, and C) were chosen for the 6-month field trial program. Three sections of the 2nd level building were chosen such that a test section covered about 4.6 m^2 surface area of a beam and a column. Each product was applied on one of the sections (Test Areas A, B, and C) according to the manufacturer's installation instructions.

Corrosion Monitoring Probes

The effectiveness of the corrosion inhibitors was evaluated by measuring instantaneous corrosion rates at four different times. These included baseline data collected just prior to corrosion inhibitor treatment and three rounds of data collection at 10 days, 89 days, and 190 days after the corrosion inhibitors were applied.

Two types of corrosion monitoring probes were used for this study. The Type I probe was constructed with a 3-electrode system and cement grout material filled the gap between the working and counter electrodes and served as a conductive electrolyte. These probes were manufactured at WJE's laboratory. Figure 1 shows a photograph of a Type I probe installed on a spandrel beam prior to covering with mortar.

Type II probes were made by electrically isolating a 3-in. long piece of #4 non-structural reinforcing bar with saw cuts through the concrete. An actual installation of a Type II probe is shown in Figure 2. The main advantage of employing Type II probes was to measure the corrosion rate of steel surrounded by the existing (undisturbed) concrete. The excavated concrete was replaced with mortar after the exposed metallic components were covered with a two-part epoxy coating.

Each structural element (beam and column) per test area contained two of each type of probe. However, the two Type II probes were replaced with Type I probes in the beam section of Test Area A due to the absence of reinforcing bars that could be cut without undermining structural integrity. All probes were installed prior to corrosion inhibitor application. Figure 3 shows a site photograph of Test Areas B and C.

In-situ Corrosion Rate Measurement

A Gamry Electrochemical Testing instrument was employed for in-situ corrosion rate measurements. The device uses the principle of linear polarization resistance from the static corrosion potential of steel. The potentiodynamic scan was made at a rate of 0.5 mV/sec between –20 mV to +20 mV with respect to the static corrosion potential of the steel sample. Tafel constants of β_a = 120 mV and β_b = 120 mV were used for calculation of the corrosion rate in the Stern-Geary equation. Figure 4 shows a corrosion rate measurement in progress. Since the Type II probes did not have built-in counter and reference electrodes, a 2-electrode system (no reference electrode) was adopted using an external stainless steel mesh as the counter

electrode/reference electrode. Due to the fluted concrete surface, a thick sponge was cut to conform to the surface shape and inserted between the counter electrode and concrete.

Trial of a Discrete Zinc Sacrificial Anode Cathodic Protection System

A discrete zinc sacrificial anode cathodic protection system was installed in the north and west side walls of an overhang trellis of the 2nd floor during the third round of corrosion rate measurements. Concrete was drilled close to the embedded reinforcing bars on a roughly 12 in. x 12 in. grid system and the proprietary zinc anodes were inserted into the holes. After the holes were patched with grout material, individual zinc anodes were electrically connected via a wire and a toggle switch to the bars.

After the anodes were installed, polarized potentials were measured on a 6 in. x 6 in. grid pattern and the total current flow from sum of the zinc anodes to the bars was measured using a digital multimeter. At the end of this testing program, total current measurements were repeated. Potentials of the test areas were also measured on the same 6 in. x 6 in. grid system under power-on, power instant-off, and 4-hour decay after power-off conditions.

TEST RESULTS AND DISCUSSION

Reduction of Corrosion Rate

Corrosion rate can be expressed by several units such as polarization resistance (R_p, ohm-cm^2), $\mu A/cm^2$, and $\mu m/yr$. It is common to use the R_p values for corrosion rate analysis since R_p of steel is inversely proportional to the corrosion rate (the higher R_p, the lower corrosion rate). In this study, R_p, and $\mu m/yr$ units were used. Corrosion rate was calculated by identifying a linear section in the experimental data points, especially in the anodic portion, and fitting the data with linear regression using the Gamry data analysis software. The fitted line determined the R_p and subsequently the corrosion rate in $\mu m/yr$. Figure 5 shows an example of low corrosion rate experimental data and a linear regression line. Data analysis indicated that the instantaneous corrosion rate was 1.1×10^7 Ω-cm^2 or 0 $\mu m/yr$. An example of high corrosion rate is shown in Figure 6. The corrosion rate of the data was determined to be 9.5×10^3 Ω-cm^2 or 32 $\mu m/yr$.

Figures 7 and 8 show the examples of polarization resistance change with time of Type I and Type II probes embedded in the test columns, respectively. Every corrosion inhibitor was able to increase the R_p (or lower the corrosion rate) soon after it was applied. At least, one order of magnitude increase in R_p was achieved initially. In general, two products exhibited better performance with further R_p increase with time, while the third product showed a gradual decrease in R_p as observed with some probes after 90 days.

Since baseline corrosion rates varied among individual probes, it was difficult to evaluate the performance with actual experimental corrosion rate data. For the sake of comparison, the corrosion rate data in terms of penetration rate were normalized by dividing all data by the relevant baseline values. Figures 9 and 10 show change in the mean values of the normalized corrosion rates (dimensionless) for Type I and Type II probes, respectively. From these two plots, it is concluded that Product A and Product C were effective at reducing the corrosion rate to a negligible state by 180 days Product C exhibited better performance than Product A when measured with Type II probes. Conversely, Product A was more effective than Product C to reduce the corrosion rates for the Type I probes. However, the performance differences between Product A and Product C were not considered significant because both products were able to reduce the corrosion rates to less than 10 percent of their baseline values in 180 days. Product B did not perform well compared to the others and was recommended not to be considered for the building.

Performance of Discrete Zinc Sacrificial Anode Cathodic Protection System

Initial galvanic currents measured in the west and north test sections were 35 mA and 17 mA, respectively. After about 100 days in testing, the current levels dropped to 4.2 mA and 3.4 mA in the same areas. Such current reduction was within the expected range as the reinforcing bars were under the constant cathodic protection. Figure 11 shows three equi-potential contour maps constructed with the last potential data collected from the west and north test sections, respectively. Figure 11(a) show the potential contour maps for the polarized state (power-on) of the test sections. As expected, steep potential gradient can be seen in the areas around the zinc anodes in the contour map. Due to high concrete resistivity, a large potential shift in the positive direction upon instant power-off can be seen in Figure 11(b).

According to the National Association of Corrosion Engineers (NACE)'s cathodic protection criteria for reinforced concrete structures, a minimum of 100 mV depolarization should be achieved between instant-off potential and the decayed potential after the cathodic protection system is off for four hours. While most area in the west test section achieved the 100 mV depolarization criteria, some spots exhibited weak depolarization indicating that the cathodic protection system might be ineffective at those spots. As shown in Figure 11(c), the entire north test section exhibited the satisfactory depolarization behavior with the magnitude well above the criteria. It was concluded that the sacrificial anode cathodic protection system could be a good corrosion mitigation option for the overhang trellis areas depending on the project requirements.

CONCLUSIONS

Based upon test results from a 6-month field evaluation of three surface-applied migrating type corrosion inhibitors and 3-month field trial of a discrete zinc sacrificial anode cathodic protection system, the following conclusions are made:

1. Product B did not perform well compared to the others and was not recommended for the building.
2. The performance differences between Product A and Product C were not considered significant because both products were able to reduce the corrosion rates to less than 10 percent of their baseline values in 180 days.
3. The discrete zinc sacrificial anode cathodic protection system could be a good corrosion mitigation option for the overhang trellis areas if the installation of the zinc anodes can ensure adequate coverage and project and economic considerations are appropriate.
4. The performance monitoring methodology employed in this study was very effective to identify and choose the best product in terms of field performance and overall cost.

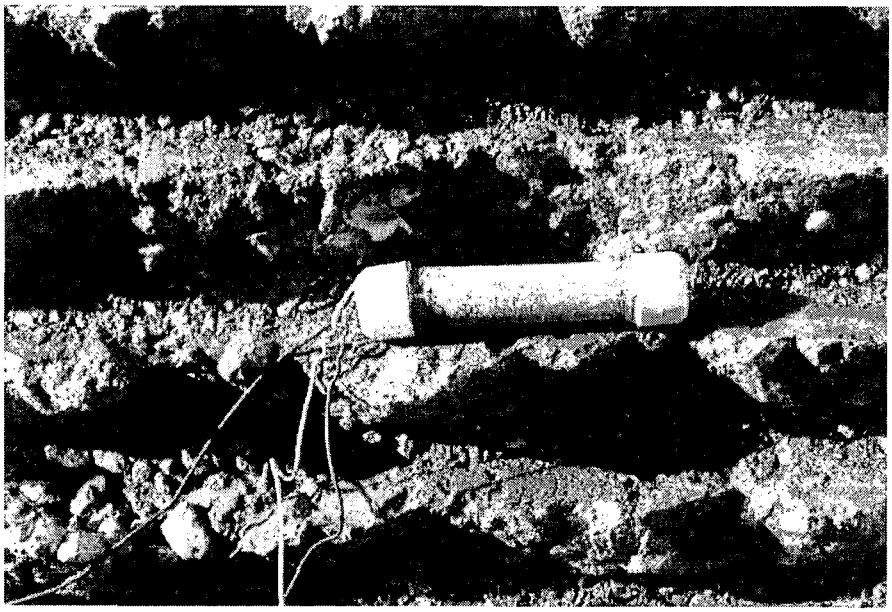

Figure 1. Photograph of Type I corrosion probe installed on a beam

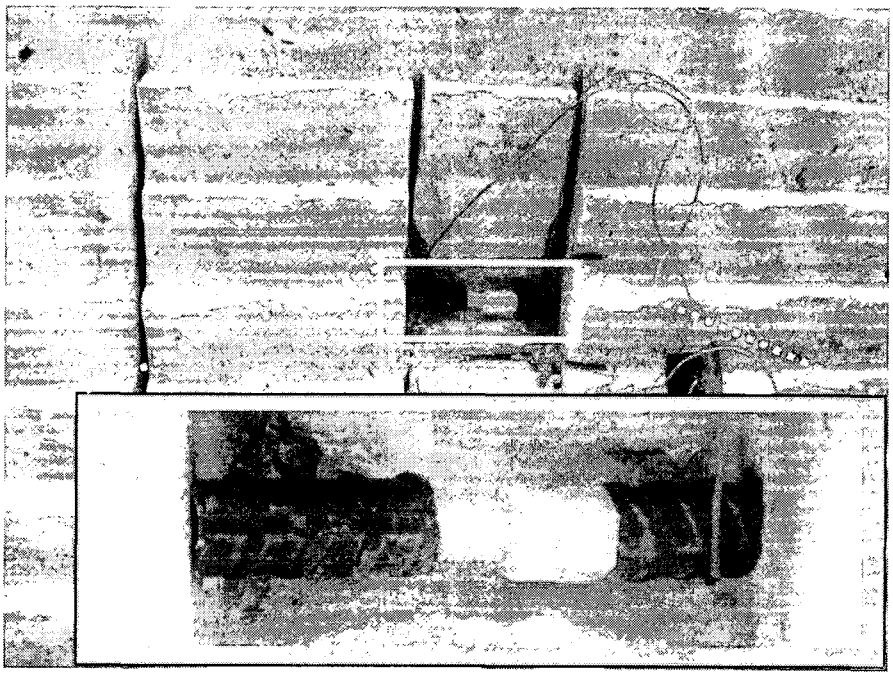

Figure 2. Photograph of Type II corrosion probe installed on a beam

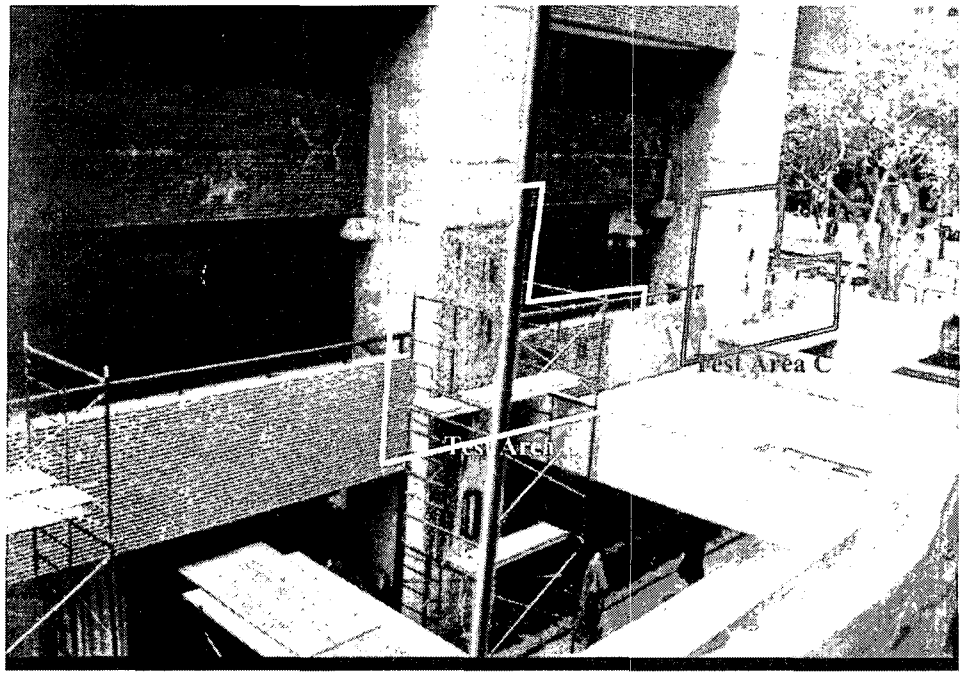

Figure 3. Another site photograph showing Test Area B treated with Product B and Test Area C treated with Product C

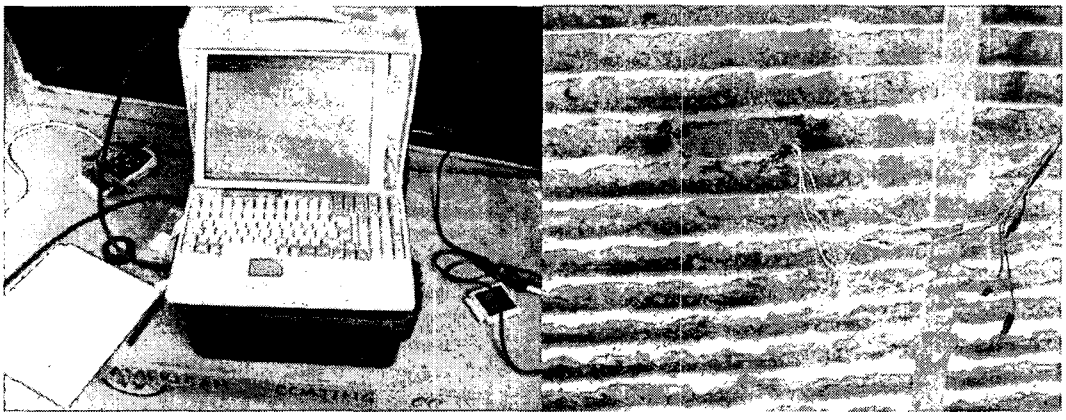

Figure 4. In-situ corrosion rate measurement using Gamry Electrochemical Testing instrument

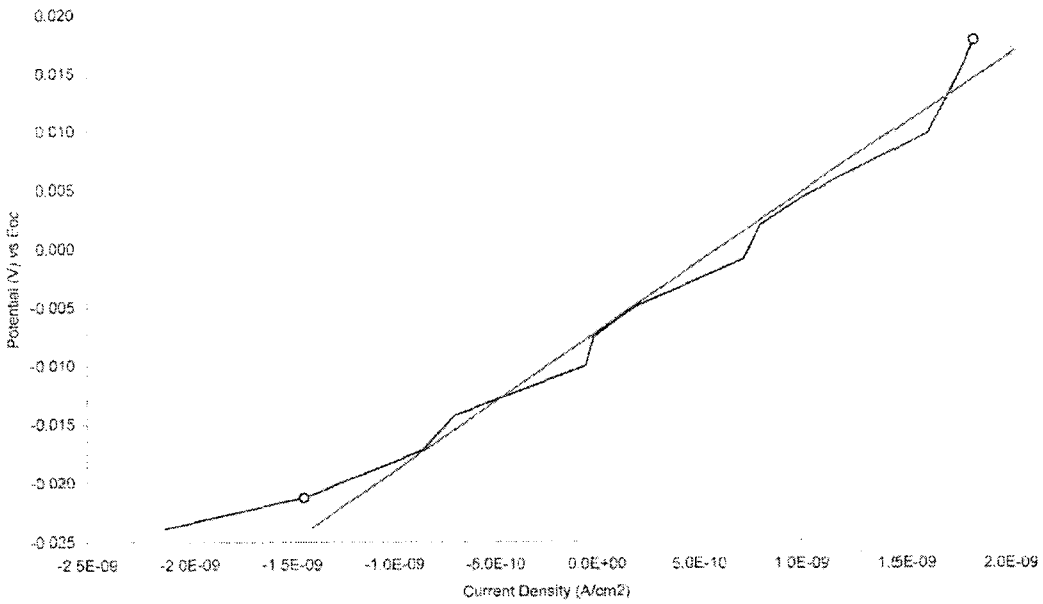

Figure 5. An example of low corrosion rate data

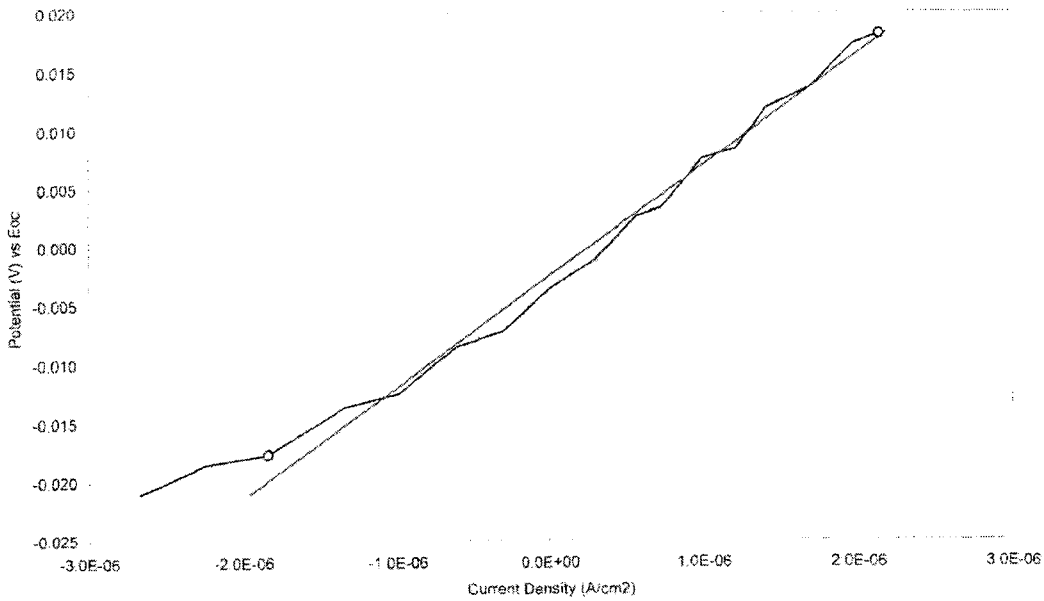

Figure 6. An example of high corrosion rate data

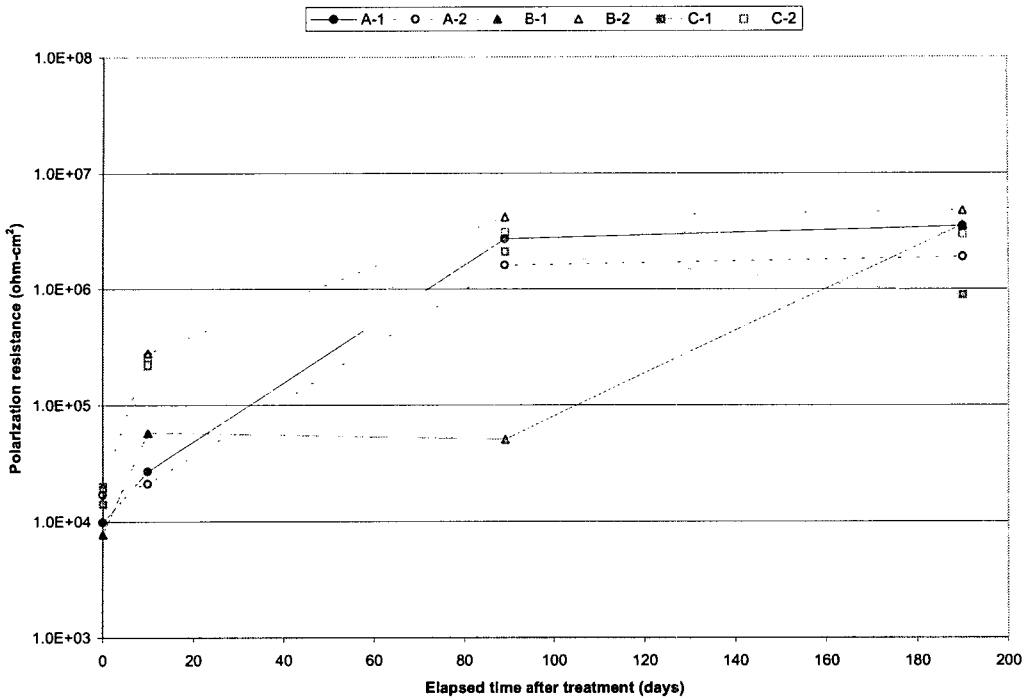

Figure 7. Change of polarization resistance with time for Type I probes embedded in the columns

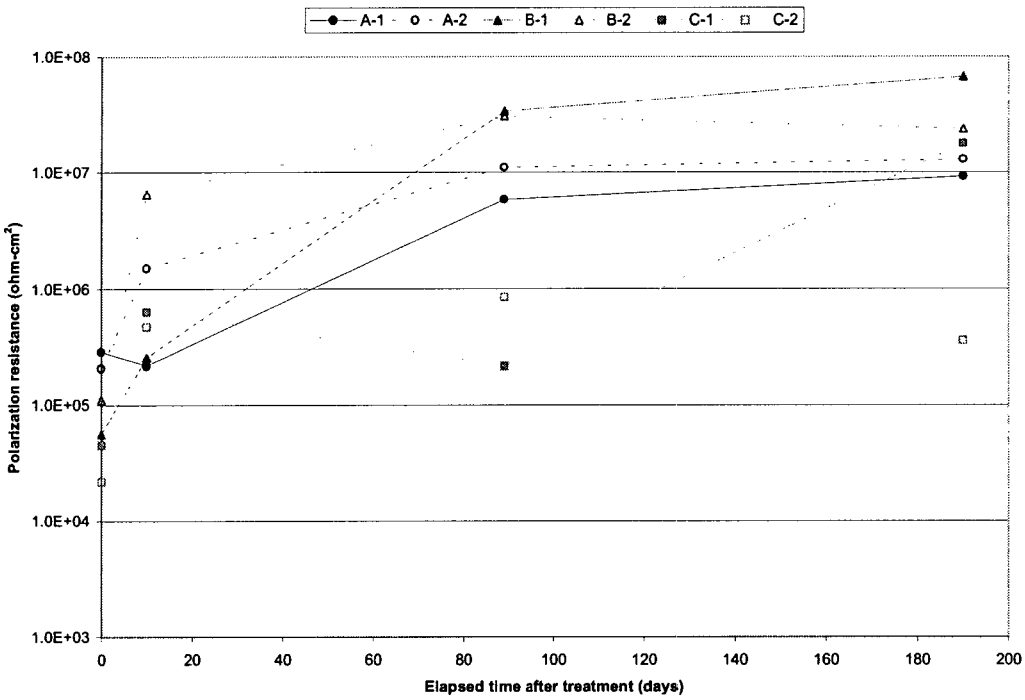

Figure 8. Change of polarization resistance with time for Type II probes in the columns

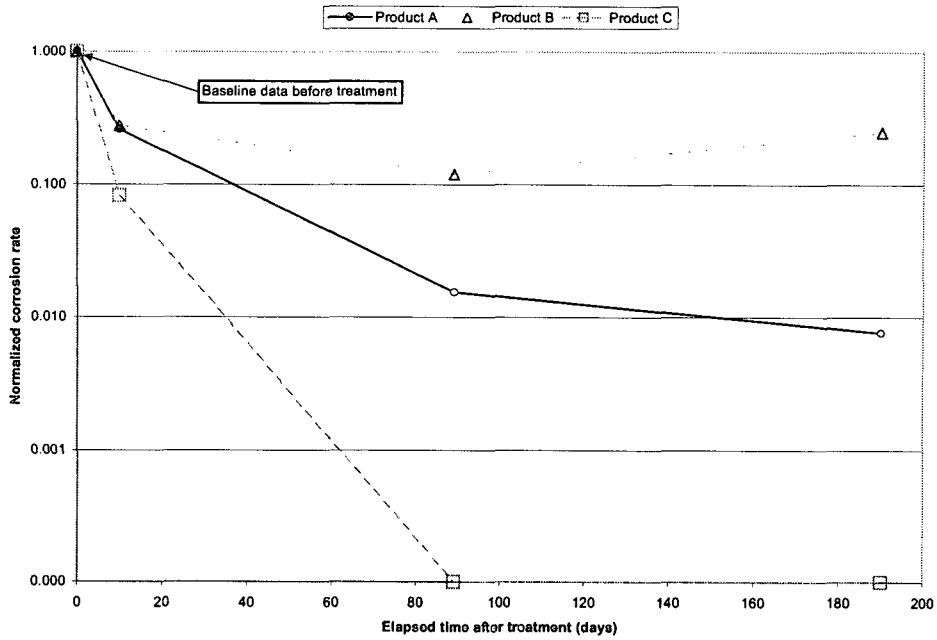

Figure 9. Change of normalized mean corrosion rates with time for Type I probes

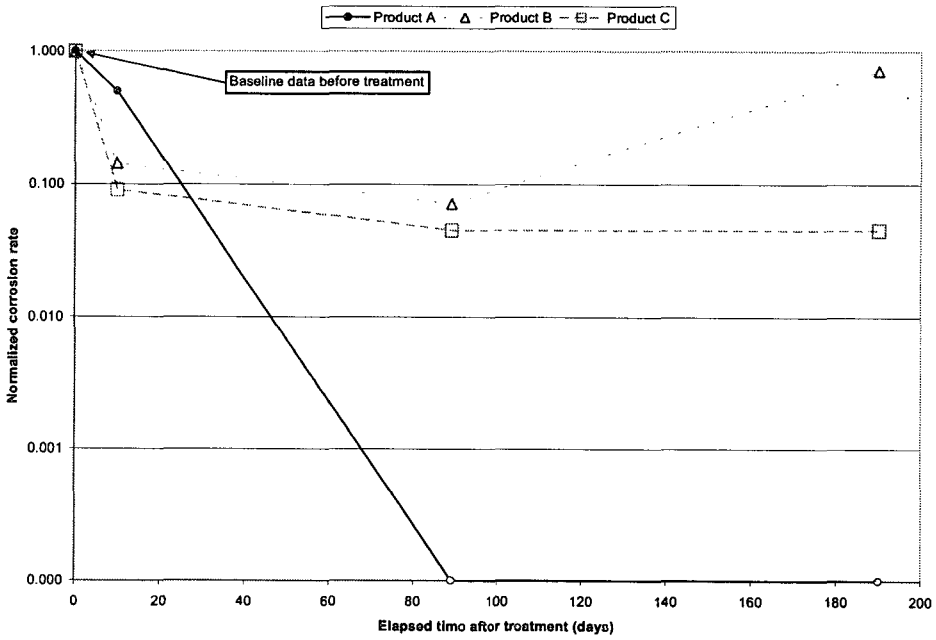

Figure 10. Change of normalized mean corrosion rates with time for Type II probes

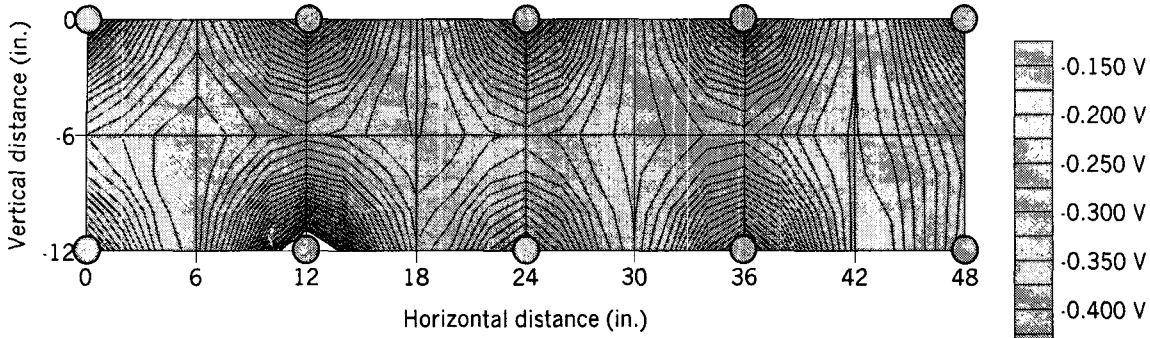

(a) Equi-potential contour map for "power-on" condition

○: Location of zinc anodes

(b) Equi-potential contour map for power "instant-off" condition

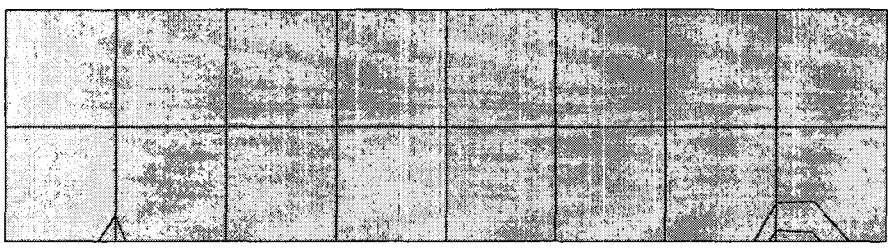

(c) Equi-potential contour map for depolarization condition

Figure 11. Performance of the zinc anodes in the north test area